

Ultrasensitive Detection of Majorana Fermions via Spin-based Optomechanics with Carbon Nanotubes

Hua-Jun Chen and Ka-Di Zhu*

Key Laboratory of Artificial Structures and Quantum Control (Ministry of Education),

Department of Physics, Shanghai Jiao Tong University,

800 DongChuan Road, Shanghai 200240, China

(Dated: October 17, 2018)

Abstract

We propose a novel optical method to detect the existence of Majorana fermions at the ends of the semiconductor nanowire via the coupling to an electron spin trapped on a carbon nanotube resonator under the control of a strong pump field and a weak probe field. The coupling strength of Majorana fermion to the spin in the carbon nanotube and the decay rate of the Majorana fermion can be easily measured from the probe absorption spectrum via manipulating the spin-mechanical coupling in the suspended carbon nanotube. The scheme proposed here will open a good perspective for its applications in all-optical controlled Majorana fermion-based quantum computation and quantum information processing.

PACS numbers: 73.21.-b, 71.10.Pm, 73.63.Fg, 62.25.-g

INTRODUCTION

Majorana fermions (MFs) proposed by Majorana[1] in 1937, with zero energy quantum particles described by hermitian second quantized operators $\gamma^\dagger = \gamma$, have attracted a great deal of one's attention due to their potential applications, e.g., topological quantum computation[2–5]. MFs, although originally proposed as a model for neutrinos, which have been detected in condensed matter systems[6–11]. It has been demonstrated that Majorana particles could exist at the ends of 1D nanowires in the presence of the appropriate superconducting pairing[10, 11] under suitable conditions. Not long ago, some researches show that using a heterostructure consisted of two conventional materials such as s-wave superconductor and semiconductor nanowire with strong spin-orbit coupling, one can generate MFs [12–16]. Although a few schemes have been proved that MFs dwell in solid state systems, experimental observation Majorana bound states (MBSs) are still a challenging, and if the direct experimental observation of Majorana particles is achieved in solid state systems, there would be a breakthrough on the research of fundamental physics and the future quantum computer[4]. Fortunately, very recently, some experiment reports have been shown that the existence of a pair of MBSs are observed at the ends of the different materials nanowire which contact with an superconductor via zero bias conductance peak[17–19] and fractional AC Josephson effect[20]. Actually, besides these schemes, MBSs could also be probed via quantum non-locality, transconductance, interference[4], and the noise measurements[21–23], as well as 4π periodic Majorana-Josephson currents[24].

Up to now, the detection of MFs in condensed matter systems based on the electrical measurements is the mainstream approach[17–20]. However, how to detect and verify the definite MBSs is still challenging[5], because the noises that may confuse the MBSs signals will be involved in the electrical measurement schemes, and they will affect the judgement whether the Majorana-like signals are true MBSs. Moreover, these methods also include the electron transfer into or out of MBSs via the nanowire, which will destroy the qubit information when MBSs are used to quantum computing. In this case, one proposes an experimental setup for detecting a Majorana zero mode by employing a single quantum dot (QD) coupled to the end of a p-wave superconducting nanowire[25, 26]. This scheme provides a potential way to probe MBSs without totally destroying the information in the qubit. Besides, Leijnse et al. present a setup to measure the lifetime of Majorana bound

states via a QD coupled to a semiconducting wire with a superconductivity[27].

On the other hand, the suspended carbon nanotubes (CNTs), due to their remarkable electronic properties, low masses and high-Q factors [28–30], attract more and more people’s attention. These advantages will make the CNTs more applicable to ultrasensitive detection and mechanical signal processing [31]. Recently, the investigation of spin-orbit interaction (SOI) in CNTs has gained significant advances, which pave the way for manipulating the spin degree of freedom [32–36]. Based on these advantages of CNTs, rather than the detection scheme[18–20, 37, 38] and what Stanescu et al.[4] elaborated, here, we shall propose a novel optical measurement scheme to detect the existence of Majorana fermion by using an electron spin trapped on a carbon nanotube resonator as a sensitive probe. We employ the optical pump-probe scheme (see Fig. 1) which has been demonstrated experimentally[39–41] to detect Majorana fermion via the probe-absorption spectrum. The vibration of CNT (i.e. the phonon cavity) enhances the probe spectrum, which makes the Majorana fermion more sensitive to be detected. Moreover, the scheme also provide a method to measure the lifetimes of Majorana fermion distinguishing the electrical measurement[27].

THEORY

The schematic setup is shown in Fig. 1, where an electron spin trapped on the suspended CNT[32] is employed to detect a pair of Majorana fermions emerged at the ends of the tunnel-coupled nanowire[18]. In the presence of a magnetic field \mathbf{B} , it constitutes a well-defined two-level spin system (TLS) with an effective spin-phonon coupling due to the interplay between SOI and flexural vibrations of the nanotube[42, 43]. The vibrational modes of nanotube resonator can be treated as phonon modes. The inset window of Fig.1 shows the two-level spin state, while dressing with the flexural modes of CNT via the spin-phonon coupling. The spin-phonon coupling mechanism is presented, where at long phonon wavelengths the deflection coupling is dominated, while at short wavelengths the deformation potential coupling should be dominated[44].

For simplicity we consider only the deflection coupling mechanism, but note that the approach can readily be extended to include both effects. The Hamiltonian describing this system is [43, 44]

$$H_{CNT} = \frac{\Delta_{so}}{2}\tau_3(\mathbf{S} \cdot \mathbf{t}) + \Delta_{KK'}\tau_1 - \mu_{orb}\tau_3(\mathbf{B} \cdot \mathbf{t}) + \mu_B(\mathbf{S} \cdot \mathbf{B}), \quad (1)$$

where Δ_{so} and $\Delta_{KK'}$ represent the curvature enhanced spin-orbit coupling and the inter-valley coupling, respectively. τ_i and S are the Pauli matrices in valley and spin space, \mathbf{t} is the tangent vector along the CNT axis, and $\mathbf{B} = B\mathbf{e}_z$ is the magnetic field along the axis of the suspended CNT. In order to study how electron spin couples to the quantized mechanical motion of the CNT, we consider only a single polarization of flexural motion, assuming that the two-fold degeneracy is broken (for example, driven by an external electric field). A generic deformation of the CNT with deflection $u(z)$ makes the tangent vector $t(z)$ coordinate-dependent. Expanding $t(z)$ for small deflections, the coupling terms in Hamiltonian (1) can be rewritten as $\mathbf{S} \cdot \mathbf{t} \simeq S_z + (du/dz)S_x$ and $\mathbf{B} \cdot \mathbf{t} \simeq B_z + (du/dz)B_x$. Expressing the deflection $u(z)$ in terms of the creation and annihilation operators a^+ and a for a quantized flexural phonon mode $u(z) = f(z)l_0(a + a^+)/\sqrt{2}$, where $f(z)$ and l_0 are the waveform and zero-point amplitude of the phonon. Thus, we obtain the Hamiltonian of the suspended CNT system as $H_{CNT} = \hbar\omega_S S^z + \hbar\omega_n a^+ a + \hbar g(S^+ a + S^- a^+)$, where $\hbar\omega_S = \mu_B(B - \Delta_{so}/2\mu_B)$, B denotes the magnetic field strength and μ_B is spin magnetic moment. ω_n is the vibrational frequency of the nanotube resonator. g is the spin-phonon coupling strength in CNT[35].

For the nanowire structure, combining a strong Rashba spin-orbit interaction and Zeeman splitting, the proximity-effect-induced s-wave superconductivity in the nanowire can support electron-hole quasiparticle excitations of MBSs at the ends of the nanowire[9, 10, 12]. Suppose the electron spin couples to γ_1 , then the Hamiltonian that describes the MBSs[11, 25, 26] is $H_1 = i\hbar\omega_M\gamma_1\gamma_2/2 + i\hbar\beta(S^- - S^+)\gamma_1$. To detect the existence of Majorana fermion, it is helpful to switch from the Majorana representation to the regular fermion one through the exact transformation $\gamma_1 = f^\dagger + f$ and $\gamma_2 = i(f^\dagger - f)$. f and f^\dagger are the fermion annihilation and creation operators obeying the anti-commutative relation $\{f, f^\dagger\} = 1$. Accordingly, H_1 can be rewritten as $H_{MBS} = \hbar\omega_M(f^\dagger f - 1/2) + i\hbar\beta(S^- f^\dagger - S^+ f)$, where the first term gives the energy of Majorana fermion at frequency ω_M , the second term describes the coupling between the right MBSs and the electron spin in CNT with the coupling strength β . Applying a strong pump field and a weak probe field to the spin of an electron simultaneously. Then the Hamiltonian of the electron spin coupled to the pump field and probe field is given by[45] $H_{S-F} = -\mu E_{pu}(S^+ e^{-i\omega_{pu}t} + S^- e^{i\omega_{pu}t}) - \mu E_{pr}(S^+ e^{-i\omega_{pr}t} + S^- e^{i\omega_{pr}t})$, where μ is the dipole moment of the electron, ω_{pu} and ω_{pr} are the frequency of the pump field and the probe field, respectively and E_{pu} (E_{pr}) is the slowly varying envelope of the pump field

(probe field). Therefore, we can obtain the total Hamiltonian of the system in the presence of two optical excitation[26, 45]. In a rotating frame at the pump field frequency ω_{pu} , the total Hamiltonian of the system can be written by

$$H = \hbar\Delta_{pu}S^z + \hbar\Delta_n a^\dagger a + \hbar\Delta_M f^\dagger f + \hbar g(S^+ a + S^- a^\dagger) + i\hbar\beta(S^- f^\dagger - S^+ f) - \hbar\Omega_{pu}(S^+ + S^-) - \mu E_{pr}(S^+ e^{-i\delta t} + S^- e^{i\delta t}), \quad (2)$$

where $\Delta_{pu} = \omega_D - \omega_{pu}$ is the detuning of the exciton frequency and the pump frequency, $\Omega_{pu} = \mu E_{pu}/\hbar$ is the Rabi frequency of the pump field, and $\delta = \omega_{pr} - \omega_{pu}$ is the probe-pump detuning. $\Delta_M = \omega_M - \omega_{pu}$ is the detuning of the Majorana fermion frequency and the pump frequency. Actually, we have neglected the regular fermion like normal electrons in the nanowire that interact with the QD in the above discuss. To describe the interaction between the normal electrons and the QD, we use the tight binding Hamiltonian of the whole wire as [46]: $H_{fs} = \hbar\omega_D S^z + \hbar \sum_k \omega_k c_k^\dagger c_k + \hbar\lambda \sum_k (c_k^\dagger S^- + S^+ c_k)$, where c_k and c_k^\dagger are the regular fermion annihilation and creation operators with energy ω_k and momentum k obeying the anti-commutative relation $\{c_k, c_k^\dagger\} = 1$, and g is the coupling strength between the normal electrons and the QD (here for simplicity we have neglected the k -dependence of g as in Ref.[47]).

According to the Heisenberg equation of motion $i\hbar dO/dt = [O, H]$ and introducing the corresponding damping and noise terms, we derive the quantum Langevin equations as follows [48, 49]

$$\dot{S}^z = -\Gamma_1(S_z + 1/2) - ig(S^+ a - S^- a^\dagger) - \beta(S^- f^\dagger + S^+ f) + i\Omega_{pu}(S^+ - S^-) + (i\mu E_{pr}/\hbar)(S^+ e^{-i\delta t} - S^- e^{i\delta t}), \quad (3)$$

$$\dot{S}^- = -(i\Delta_{pu} + \Gamma_2)S^- + 2(\beta f + iga)S^z - 2i\Omega_{pu}S^z - 2i\mu E_{pr}S^z e^{-i\delta t}/\hbar + \hat{F}_{in}(t), \quad (4)$$

$$\dot{f} = -(i\Delta_M + \kappa_M/2)f + \beta S^- + \hat{\xi}_M(t), \quad (5)$$

$$\dot{a} = -(i\Delta_n + \kappa/2)a - igS^- + \hat{\xi}(t), \quad (6)$$

where Γ_1 and Γ_2 are the electron spontaneous emission rate and dephasing rate, κ is the decay rate of CNT and κ_M is the decay rate of the Majorana fermion. $\hat{F}_{in}(t)$ is the δ -correlated Langevin noise operator, which has zero mean $\langle \hat{F}_{in}(t) \rangle = 0$ and obeys the correlation function $\langle \hat{F}_{in}(t) \hat{F}_{in}^\dagger(t') \rangle \sim \delta(t - t')$. The resonator mode of CNT is affected by a Brownian stochastic force with zero mean value, and $\hat{\xi}(t)$ has the correlation function

$\langle \hat{\xi}^+(t)\hat{\xi}(t') \rangle = \frac{\kappa}{\omega_n} \int \frac{d\omega}{2\pi} \omega e^{-i\omega(t-t')} [1 + \coth(\frac{\hbar\omega}{2k_B T})]$, where k_B and T are the Boltzmann constant and the temperature of the reservoir of the coupled system. Majorana fermion has the same correlation relation as resonator mode of CNT.

To go beyond weak coupling, the Heisenberg operator can be rewritten as the sum of its steady-state mean value and a small fluctuation with zero mean value: $S^z = S_0^z + \delta S^z$, $S^- = S_0^- + \delta S^-$, $f = f_0 + \delta f$ and $a = a_0 + \delta a$. Since the driving fields are weak, but classical coherent fields, we will identify all operators with their expectation values, and drop the quantum and thermal noise terms[39, 49]. Simultaneously inserting these operators into the Langevin equations Eqs. (3)-(6) and neglecting the nonlinear term $\delta f \delta S^-$, $\delta a \delta S^-$, $\delta S^z \delta f$ and $\delta S^z \delta a$, the linearized Langevin equations can be written as:

$$\begin{aligned} \langle \delta \dot{S}^z \rangle &= -\Gamma_1 \langle \delta S^z \rangle - \beta(S_0^- \langle \delta f^+ \rangle + f_0^* \langle \delta S^- \rangle + S_0^{-*} \langle \delta f \rangle + f_0 \langle \delta S^+ \rangle) \\ &\quad - ig(S_0^{-*} \langle \delta a \rangle + a_0 \langle \delta S^+ \rangle - S_0^- \langle \delta a^+ \rangle - a_0^* \langle \delta S^- \rangle) + i\Omega_{pu}(\langle \delta S^+ \rangle - \langle \delta S^- \rangle) \\ &\quad + (i\mu E_{pr}/\hbar)(S_0^{-*} e^{-i\delta t} - S_0^- e^{i\delta t}), \end{aligned} \quad (7)$$

$$\begin{aligned} \langle \delta \dot{S}^- \rangle &= -(i\Delta_{pu} + \Gamma_2) \langle \delta S^- \rangle + 2\beta(S_0^z \langle \delta f \rangle + f_0 \langle \delta S^z \rangle) + 2ig(S_0^z \langle \delta a \rangle + a_0 \langle \delta S^z \rangle) \\ &\quad - 2i\Omega_{pu} \langle \delta S^z \rangle - 2i\mu E_{pr} S_0^z e^{-i\delta t} / \hbar, \end{aligned} \quad (8)$$

$$\langle \delta \dot{f} \rangle = -(i\Delta_M + \kappa_M/2) \langle \delta f \rangle + \beta \langle \delta S^- \rangle, \quad (9)$$

$$\langle \delta \dot{a} \rangle = -(i\Delta_n + \kappa/2) \langle \delta a \rangle - ig \langle \delta S^- \rangle, \quad (10)$$

accordingly, we can obtain the corresponding steady-state equations and from these equations we get: $\Gamma_1(w_0 + 1)\{(\Delta_{pu}^2 + \Gamma_2^2)(\Delta_M^2 + \kappa_M^2/4)(\Delta_n^2 + \kappa^2/4) + w_0^2[g^4(\Delta_M^2 + \kappa_M^2/4) + \beta^2(\Delta_n^2 + \kappa^2/4) + g^2\beta^2(2\Delta_M\Delta_n + \kappa_M\kappa/4)] + w_0[g^2(\Delta_M^2 + \kappa_M^2/4)(2\Delta_{pu}\Delta_M - \Gamma_2\kappa_M) + \beta^2(2\Delta_{pu}\Delta_M + \Gamma_2\kappa_M)]\} - 2\Omega_{pu}^2 w_0[3\kappa g^2(\Delta_M^2 + \kappa_M^2/4) + \kappa_M\beta^2(\Delta_n^2 + \kappa^2/4)] + 4\Omega_{pu}^2 w_0\Gamma_2(\Delta_M^2 + \kappa_M^2/4)(\Delta_n^2 + \kappa^2/4) = 0$ which determines the population inversion ($w_0 = 2S_0^z$) of the electron in CNT.

In order to solve Eqs. (7)-(10), we make the ansatz[45] $\langle \delta S^z \rangle = S_+^z e^{-i\delta t} + S_-^z e^{i\delta t}$, $\langle \delta S^- \rangle = S_+ e^{-i\delta t} + S_- e^{i\delta t}$, $\langle \delta f \rangle = f_+ e^{-i\delta t} + f_- e^{i\delta t}$ and $\langle \delta a \rangle = a_+ e^{-i\delta t} + a_- e^{i\delta t}$. Substituting these equations into Eqs. (7)-(10), and working to the lowest order in E_{pr} but to all orders in E_{pu} , we can obtain the linear susceptibility as $\chi_{eff}^{(1)}(\omega_{pr}) = \mu S_+(\omega_{pr})/E_{pr} = (\mu^2/\hbar)\chi^{(1)}(\omega_{pr})$, where $\chi^{(1)}(\omega_{pr})$ is given by

$$\chi^{(1)}(\omega_{pr}) = \frac{(d_4^* - h_2 d_3^*)d_1 h_3 - i w_0 d_4^* \Gamma_2}{d_2 d_4^* - h_1 h_3 d_1 d_3^*} \Gamma_2, \quad (11)$$

where f_0 , S_0^- and a_0 can be derived from the steady-state equations and $b_1 = \beta/(i\Delta_M + \kappa_M/2 - i\delta)$, $b_2 = \beta/(i\Delta_M + \kappa_M/2 + i\delta)$, $b_3 = -ig/(i\Delta_n + \kappa/2 - i\delta)$, $b_4 = -ig/(i\Delta + \kappa/2 + i\delta)$, $h_1 = [-ig(S_0^{-*}b_3 - a_0^*) - \beta(f_0^* + S_0^{-*}b_1) - i\Omega_{pu}]/(\Gamma_1 - i\delta)$, $h_2 = [-ig(a_0 - S_0^-b_4^*) - \beta(S_0^-b_2^* + f_0) + i\Omega_{pu}]/(\Gamma_1 - i\delta)$, $h_3 = iS_0^{-*}/(\Gamma_1 - i\delta)$, $d_1 = 2(iga_0 - i\Omega_{pu} + \beta f_0)$, $d_2 = i\Delta_{pu} + \Gamma_2 - i\delta - (igb_3 + \beta b_1)w_0 - d_1h_1$, $d_3 = 2(iga_0 - i\Omega_{pu} + \beta f_0)$, $d_4 = i\Delta_{pu} + \Gamma_2 + i\delta - (igb_4 + \beta b_2)w_0 - d_3h_4$ (where O^* indicates the conjugate of O). The quantum Langevin equations of the normal electrons coupled to CNT have the same form as Majorana fermions, therefore, we omit its derivation and only give the results in the following section.

RESULTS AND DISCUSSIONS

The electron with spin trapped inside the center of CNT couples to the nearby Majorana fermion in InSb nanowire in the simultaneous presence of a strong pump beam and a weak probe beam as shown in Fig.1. For illustration of the numerical results, here we use the realistic experimental parameters[32, 35, 50]: $\kappa = 0.05MHz$, $\Gamma_1 = 0.1MHz$, $\Gamma_2 = \Gamma_1/2$ and the coupling strength between the electron spin and the nanotube vibrational mode $g = 2\pi \times 0.56MHz$. For Majorana fermion, there are no experimental values for the lifetime of the Majorana fermion and the coupling strength between the electron spin and Majorana bound states as far as we know. However, according to a few reports [16–20], we assume that the order of magnitudes of these two parameters are in the range of megahertz, while in our letter, we consider the coupling strength $\beta = 0.2MHz$ and the lifetime of the Majorana fermion $\kappa_M = 0.1MHz$. When the electron spin in CNT couples to the nearby MBS and produces the coupled states $|ex, n_M\rangle$ and $|ex, n_M + 1\rangle$ (n_M denotes the number states of the Majorana bound states) as shown in the inset of Fig. 1.

When radiating a strong pump field and a weak probe field on this system, we can detect the existence of a Majorana fermion via the coupling between Majorana bound states and the electron spin in CNT from the probe absorption spectrum. Fig. 2(a) shows the absorption spectrum of the probe field (i.e., the imaginary part of the dimensionless susceptibility $Im\chi^{(1)}$) as a function of the probe-spin detuning Δ_{pr} ($\Delta_{pr} = \omega_{pr} - \omega_S$) with several different coupling strengths β . The black solid curve is the result when no Majorana bound states exists in the nanowire. As Majorana bound states appears at the ends of the nanowire, the electron spin in CNT will couple to the right Majorana bound states, which induces the

upper level of the state $|ex\rangle$ to split into $|ex, n_M\rangle$ and $|ex, n_M + 1\rangle$. The two peaks presented in Fig. 2(a) with a given coupling strength β indicate the spin-MBS interaction. As shown in the low two insets of Fig. 2(a), the left peak signifies the transition from $|g\rangle$ to $|ex, n_M\rangle$ while the right peak is due to the transition of $|g\rangle$ to $|ex, n_M + 1\rangle$. To determine this signature is the true Majorana bound states that appear in the nanowire, rather than the normal electrons that couple with the QD, we give the numerical results of the normal electrons in the nanowire that couple with the QD as shown in the upper right inset of Fig.2(a). In order to compare with the Majorana signature, the parameters are chosen the same as Majorana fermion's parameters. We find that there is no signal in the probe absorption spectrum (see the red solid line in the inset of Fig.2(a)) which means that the splitting of the probe absorption spectrum is the true signature of MBS. Therefore, our result here reveals that the splitting in the probe absorption is a real signature of MBS, and the stronger coupling strength introduces the wider and deeper dip. Furthermore, the distance of the splitting becomes larger and larger with increasing the coupling strength β , which obviously reveals the spin-MBSs coupling. From Fig. 2(b) we find that the distance of the splitting is twice times larger than the spin-MBSs coupling strength, which provides a concise way to measure the spin-MBS coupling strength in this coupled system. In Fig. 2(b), we give a linear relationship between the distance of the peak splitting and the spin-MBS coupling strength. Therefore, the coupling strength can be obtained immediately by directly measuring the distance of two peaks in the probe absorption spectrum.

Fig. 3 demonstrates the behavior of the lifetime of the Majorana fermion when the pump field is resonant with the frequency of the electron spin in CNT. In Fig. 3, we plot the relationship between the transmission and the lifetime of the Majorana fermion. It shows that the transmission of the probe field decreases with the increase of the decay rate of the Majorana fermion. This figure provides us a simple method to measure the decay rate of the Majorana fermion. Through this method, we can determine the decay rate of the Majorana fermion and further investigate its relation with the environment via the transmission spectrum of the probe field.

In order to demonstrate the function of the vibration in CNT, we plot Fig. 4. Fig. 4 presents the absorption spectrum of the probe field as a function of the probe detuning Δ_{pr} with different coupling strengths g . In Fig. 4, three couplings strength $g = 0, 0.2, 0.56MHz$ are considered. $g = 0$ means that there is no spin-phonon coupling in the suspended CNT,

the two sharp peaks in the absorption spectrum still appear. However, once the spin-phonon coupling turns on and increases the coupling to the realistic experimental value $g = 0.56MHz$ [32], the two peaks of the absorption spectrum becomes more significant than that without the spin-phonon coupling in CNT, which means that the vibration of CNT (i.e. the phonon cavity) enhances the probe spectrum and makes the Majorana fermion more sensitive to be detected. This phonon cavity enhanced effect is analogous to the optical cavity enhanced effect in quantum optics[52].

CONCLUSIONS

In conclusion, a novel scheme which consists of an electron spin trapped on the suspended carbon nanotube and a tunnel-coupled semiconductor nanowire for demonstrating the existence of a Majorana fermion is proposed according to spin-based optomechanics. Based on this scheme, we propose a simple method to determine the interaction constant of the spin-Majorana bound states and the decay rate of the Majorana fermion via the probe absorption spectrum. Due to the phonon cavity enhanced effect, the Majorana fermion becomes more and more easier to be detected in this coupled system. Our scheme proposed here may provide us a potential application in all-optical controlled Majorana fermion based quantum computer and quantum information processing.

ACKNOWLEDGMENTS

The authors gratefully acknowledge support from the National Natural Science Foundation of China (No.10974133 and No.11274230), the National Ministry of Education Program for PhD and the National Basic Research Program of the Ministry of Science and Technology of China.

References

* Electronic address: zhukadi@sjtu.edu.cn

- [1] Majorana E 1937 *Nuovo Cimento* **14** 171
- [2] Alicea J 2012 *Rep. Prog. Phys.* **75** 076501
- [3] Beenakker C W J 2013 *Annu. Rev. Condens. Matter Phys.* **4** 113
- [4] D. S. Tudor and T. Sumanta arXiv: 1302.5433.
- [5] Franz M arXiv: 1302.3641
- [6] Sarma S D, Freedman M and Nayak C 2005 *Phys. Rev. Lett.* **94** 166802
- [7] Stern A and Halperin B I 2006 *Phys. Rev. Lett.* **96** 016802
- [8] Bonderson P, Kitaev A and Shtengel K 2006 *Phys. Rev. Lett.* **96** 016803
- [9] Lutchyn R M, Sau J D and Sarma S D 2010 *Phys. Rev. Lett.* **105** 077001
- [10] Oreg Y, Refael G and von Oppen F 2010 *Phys. Rev. Lett.* **105** 177002
- [11] Sau J D, Lutchyn R M, Tewari S and Sarma S D 2010 *Phys. Rev. Lett.* **104** 040502
- [12] Sau J D, Tewari S and Sarma S D 2012 *Phys. Rev. B* **85** 064512
- [13] Sau J D, Tewari S, Lutchyn R M, Stanescu T D and S. D. Sarma S D 2010 *Phys. Rev. B* **82** 214509
- [14] Alicea J 2010 *Phys. Rev. B* **81** 125318
- [15] Potter A C and Lee P L 2010 *Phys. Rev. Lett.* **105** 227003
- [16] Mao L, Gong M, Dumitrescu E, Tewari S and Zhang C 2012 *Phys. Rev. Lett.* **108** 177001
- [17] Deng M T, Yu C L, Huang G Y, Larsson M, Caroff P and Xu H Q 2012 *Nano Lett.* **12** 6414
- [18] Mourik V, Zuo K, Frolov S M, Plissard S R, Bakkers E P A M and Kouwenhoven L P 2012 *Science* **336** 1003
- [19] Das A, Ronen Y, Most Y, Oreg Y, Heiblum M and Shtrikman H 2012 *Nature Phys.* **8** 887
- [20] Rokhinson L P, Liu X Y and Furdyna J K 2012 *Nature Phys.* **8** 795
- [21] Bolech C J and Demler E 2007 *Phys. Rev. Lett.* **98** 237002
- [22] Nilsson J, Akhmerov A R and Beenakker C W J 2008 *Phys. Rev. Lett.* **101** 120403
- [23] Law K T, Lee P A and Ng T K 2009 *Phys. Rev. Lett.* **103** 237001
- [24] Fu L and Kane C L 2009 *Phys. Rev. B* **79** 161408
- [25] Liu D E and Baranger H U 2011 *Phys. Rev. B* **84** 201308

- [26] Cao Y S, Wang P Y, Xiong G, Gong M and Li X-Q 2012 *Phys. Rev. B* **86** 115311
- [27] Leijnse M and Flensberg K 2011 *Phys. Rev. B* **84** 140501(R)
- [28] Witkamp B, Poot M and van der Zant H S J 2006 *Nano Lett.* **6** 2904
- [29] Jespersen T S, Grove-Rasmussen K, Paaske J, Muraki K, Fujisawa T, Nygård J and Flensberg K 2011 *Nature Phys.* **7** 384
- [30] Eichler A, Moser J, Chaste J, Zdrojek M, Wilson-Rae I and Bachtold A 2011 *Nature Nanotechnol.* **6** 339
- [31] Lassagne B, Tarakanov Y, Kinaret J, Garcia-Sanchez D and Bachtold A 2009 *Science* **325** 1107
- [32] Kuemmeth F, Ilani S, Ralph D C and McEuen P L 2008 *Nature* **452** 448
- [33] Arcizet O, Jacques V, Siria A, Poncharal P, Vincent P and Seidelin S 2011 *Nature Phys.* **7** 879
- [34] Kuemmeth F, Churchill H O H, Herring P K and Marcus C M 2010 *Mater. Today* **13** 18
- [35] Pályi A, Struck P R, Rudner M, Flensberg K and Burkard G 2012 *Phys. Rev. Lett.* **108** 206811
- [36] Li J-J and Zhu K-D 2012 *Sci. Rep.* **2** 903
- [37] Benjamin C and Pachos J K 2010 *Phys. Rev. B* **81** 085101
- [38] Walter S, Schmidt T L, Børkje K and Trauzettel B 2011 *Phys. Rev. B* **84** 224510
- [39] Weis S, Rivière R, Deleglise S, Gavartin E, Arcizet O, Schliesser A and Kippenberg T J 2010 *Science* **330** 1520
- [40] Teufel J D, Li D, Allman M S, Cicak K, Sirois A J, Whittaker J D and Simmonds R W 2011 *Nature* **471** 204
- [41] Safavi-Naeini A H, Mayer Alegre T P, Chan J, Eichenfield M, Winger M, Lin Q, Hill J T, Chang D E and Painter O 2011 *Nature* **472** 69
- [42] Ohm C, Stampfer C, Splettstoesser J and Wegewijs M R 2012 *Appl. Phys. Lett.* **100** 143103
- [43] Flensberg K and Marcus C M 2012 *Phys. Rev. B* **81** 195418
- [44] Rudner M S and Rashba E I 2012 *Phys. Rev. B* **81** 125426
- [45] Boyd R W 1992 *Nonlinear Optics* (Academic, San Diego: CA) pp 225
- [46] G.D.Mahan, Many-Particle Physics (Plenum Press, New York, 1992).
- [47] A.C.Hewson, The Kondo Problem to Heavy Fermions (Cambridge University Press, New York, 1993).
- [48] Gardiner C W and Zoller P 2000 *Quantum Noise* (Springer, Berlin) pp 425–433

- [49] Walls D F and Milburn G J 1994 *Quantum Optics* (Springer, Berlin) pp 245–265
- [50] Steele G A, Hüttel A K, Witkamp B, Poot M, Meerwaldt H B, Kouwenhoven L P and van der Zant H S J 2009 *Science* **325** 1103
- [51] Fleischhauer M, Imamoglu A, Marangos J P 2005 *Rev. Mod. Phys.* **77** 633
- [52] Stapfner S, Ost L, Hunger D, Weig E M, Reichel J and Favero I arXiv:1211.1608.

Figure Captions

FIG.1 Schematic setup for detecting a Majorana fermion through an electron spin trapped on the suspended CNT coupled to a semiconductor nanowire contacting with a s-wave superconductor in the simultaneous presence of a strong pump field and a weak probe field. The inset is an energy-level diagram of the electron spin coupled to Majorana fermion in semiconductor nanowire and the vibrational motion in CNT.

FIG.2 (a) The probe absorption spectrum as a function of detuning Δ_{pr} with several different spin-MBS coupling strengths. The black solid line is the result for $\beta = 0\text{MHz}$ and $\lambda = 0\text{MHz}$. The upper right inset is the normal electrons in the nanowire that couple with the CNT at the coupling strength $\lambda = 0.3\text{MHz}$ and the spin-MBS coupling strength $\beta = 0.3\text{MHz}$. The low two insets represents the energy level transitions of the left peak and right peak presented in the absorption spectrum. (b) The linear relationship between the distance of peak splitting and the coupling strength of spin-MBS. The parameters used are $\Gamma_1 = 0.1\text{MHz}$, $\Gamma_2 = \Gamma_1/2$, $\kappa_M = 0.1\text{MHz}$, $\kappa = 0.05\text{MHz}$, $g = 0\text{MHz}$, $\Delta_M = -0.1\text{MHz}$, $\Omega_{pu}^2 = 7 \times 10^{-4}(\text{MHz})^2$ and $\Delta_{pu} = \Delta_n = 0$.

FIG.3 The transmission of a probe beam as a function of the lifetime of Majorana fermion. The parameters used are $\Gamma_1 = 0.1\text{MHz}$, $\Gamma_2 = \Gamma_1/2$, $\beta = 0.3\text{MHz}$, $\kappa = 0.05\text{MHz}$, $g = 0\text{MHz}$, $\Delta_M = -0.1\text{MHz}$, $\Omega_{pu}^2 = 7 \times 10^{-4}(\text{MHz})^2$ and $\Delta_{pu} = \Delta_n = 0$.

FIG.4 The probe absorption spectrum as a function of detuning Δ_{pr} with three different spin-phonon coupling strengths $g = 0, 0.2, 0.56\text{MHz}$. The parameters used are the same as in FIG.3.

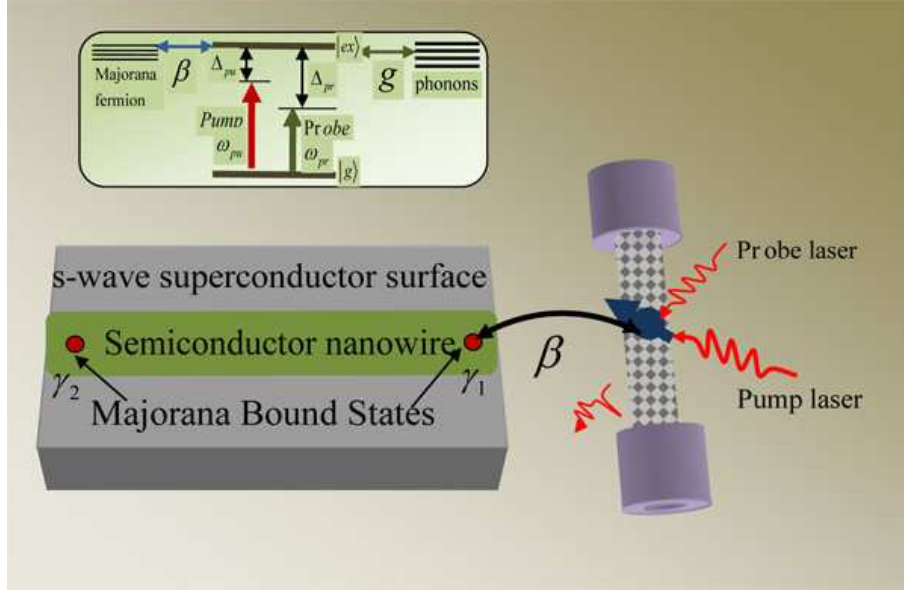


FIG. 1: Schematic setup for detecting a Majorana fermion through an electron spin trapped on the suspended CNT coupled to a semiconductor nanowire contacting with a s-wave superconductor in the simultaneous presence of a strong pump field and a weak probe field. The inset is an energy-level diagram of the electron spin coupled to Majorana fermion in semiconductor nanowire and the vibrational motion in CNT.

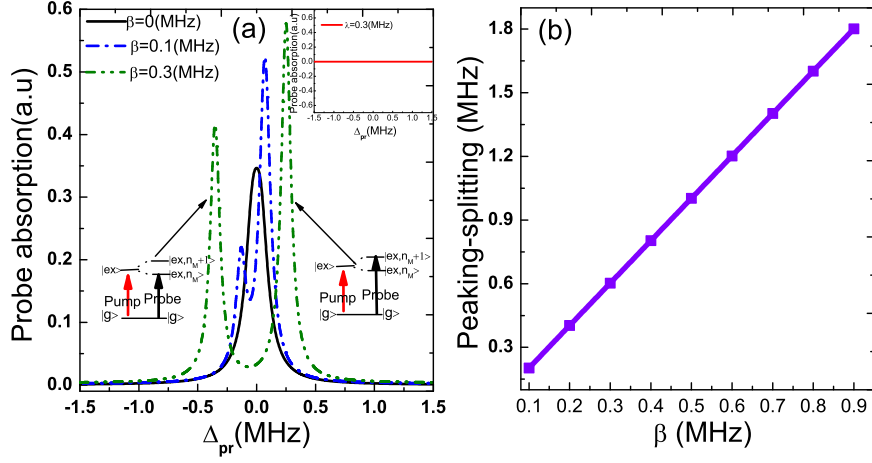


FIG. 2: (a) The probe absorption spectrum as a function of detuning Δ_{pr} with several different spin-MBS coupling strengths. The black solid line is the result for $\beta = 0$ MHz and $\lambda = 0$ MHz. The upper right inset is the normal electrons in the nanowire that couple with the CNT at the coupling strength $\lambda = 0.3$ MHz and the spin-MBS coupling strength $\beta = 0.3$ MHz. The low two insets represents the energy level transitions of the left peak and right peak presented in the absorption spectrum. (b) The linear relationship between the distance of peak splitting and the coupling strength of spin-MBS. The parameters used are $\Gamma_1 = 0.1$ MHz, $\Gamma_2 = \Gamma_1/2$, $\kappa_M = 0.1$ MHz, $\kappa = 0.05$ MHz, $g = 0$ MHz, $\Delta_M = -0.1$ MHz, $\Omega_{pu}^2 = 7 \times 10^{-4} (\text{MHz})^2$ and $\Delta_{pu} = \Delta_n = 0$.

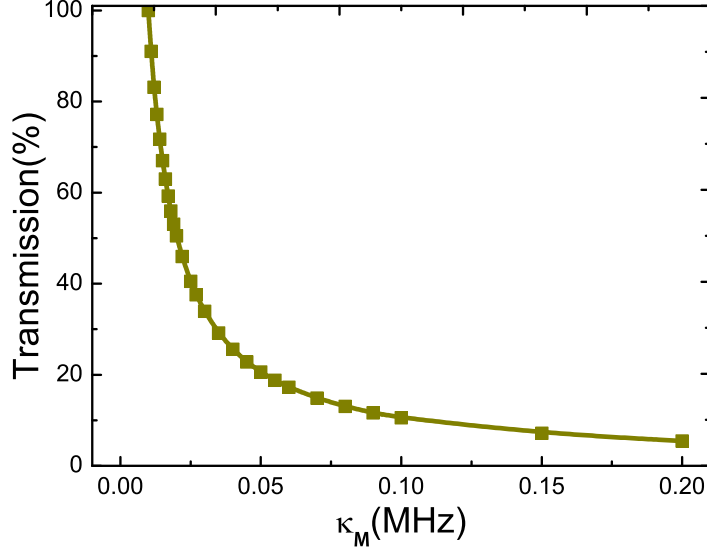


FIG. 3: The transmission of a probe beam as a function of the lifetime of Majorana fermion. The parameters used are $\Gamma_1 = 0.1\text{MHz}$, $\Gamma_2 = \Gamma_1/2$, $\beta = 0.3\text{MHz}$, $\kappa = 0.05\text{MHz}$, $g = 0\text{MHz}$, $\Delta_M = -0.1\text{MHz}$, $\Omega_{pu}^2 = 7 \times 10^{-4}(\text{MHz})^2$ and $\Delta_{pu} = \Delta_n = 0$.

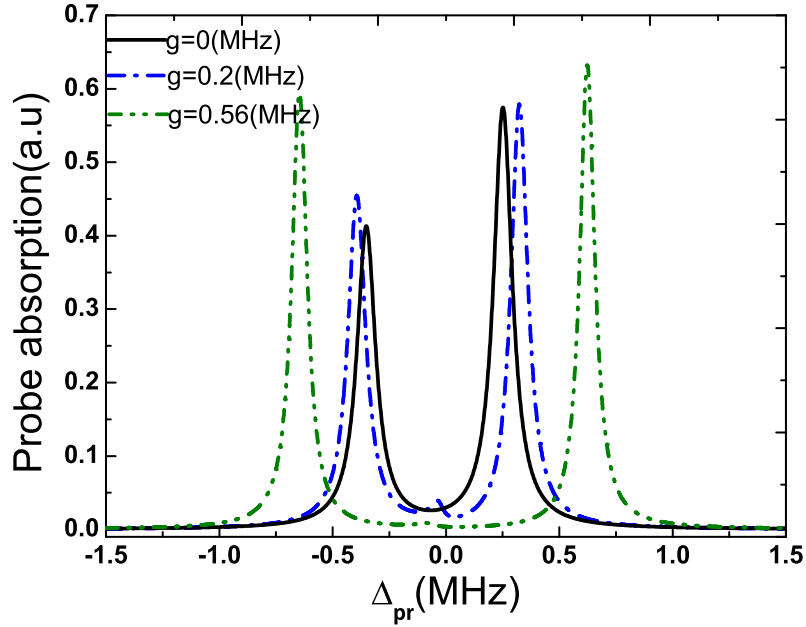


FIG. 4: The probe absorption spectrum as a function of detuning Δ_{pr} with three different spin-phonon coupling strengths $g = 0, 0.2, 0.56\text{MHz}$. The parameters used are the same as in FIG.3.